Published in final edited form as:

Int J Radiat Oncol Biol Phys. 2015 November 1; 93(3): 577–587. doi:10.1016/j.ijrobp.2015.07.2274.

Definitive Management of Oligometastatic Melanoma in a Murine Model Using Combined Ablative Radiation Therapy and Viral Immunotherapy

Miran Blanchard, MD[*,†], **Kevin G. Shim, BS**[*,‡], **Michael P. Grams, PhD**[†], **Karishma Rajani, PhD**[*], **Rosa M. Diaz, PhD**[*], **Keith M. Furutani, PhD**[†], **Jill Thompson, AAS**[*], **Kenneth R. Olivier, MD**[†], **Sean S. Park, MD, PhD**[†], **Svetomir N. Markovic, MD, PhD**[‡,§], **Hardev Pandha, MD, PhD**[‖], **Alan Melcher, PhD**[¶], **Kevin Harrington, PhD**[#], **Shane Zaidi, PhD**[*,#], and **Richard Vile, PhD**[*,‡,¶]

[*]Department of Molecular Medicine, Mayo Clinic, Rochester, Minnesota

[†]Department of Radiation Oncology, Mayo Clinic, Rochester, Minnesota

[‡]Department of Immunology, Mayo Clinic, Rochester, Minnesota

[§]Department of Medical Oncology, Mayo Clinic, Rochester, Minnesota

[‖]The Postgraduate Medical School, University of Surrey, Guildford, United Kingdom

[¶]Leeds Institute of Cancer Studies and Pathology, University of Leeds, Leeds, United Kingdom

[#]Targeted Therapy Laboratory, The Institute of Cancer Research, London, United Kingdom

Abstract

Purpose—The oligometastatic state is an intermediate state between a malignancy that can be completely eradicated with conventional modalities and one in which a palliative approach is undertaken. Clinically, high rates of local tumor control are possible with stereotactic ablative radiation therapy (SABR), using precisely targeted, high-dose, low-fraction radiation therapy. However, in oligometastatic melanoma, virtually all patients develop progression systemically at sites not initially treated with ablative radiation therapy that cannot be managed with conventional chemotherapy and immunotherapy. We have demonstrated in mice that intravenous administration of vesicular stomatitis virus (VSV) expressing defined tumor-associated antigens (TAAs) generates systemic immune responses capable of clearing established tumors. Therefore, in the present preclinical study, we tested whether the combination of systemic VSV-mediated antigen delivery and SABR would be effective against oligometastatic disease.

Methods and Materials—We generated a model of oligometastatic melanoma in C57BL/6 immunocompetent mice and then used a combination of SABR and systemically administered VSV-TAA viral immunotherapy to treat both local and systemic disease.

Reprint requests to: Richard Vile, PhD, Departments of Molecular Medicine and Immunology, Mayo Clinic, Gugg 18, 200 First St SW, Rochester, MN 55905. Tel: (507) 284-3178; ; Email: vile.richard@mayo.edu

M. Blanchard and K.G. Shim contributed equally.

S. Zaidi and R. Vile are joint senior authors.

Conflict of interest: none.

Results—Our data showed that SABR generates excellent control or cure of local, clinically detectable, and accessible tumor through direct cell ablation. Also, the immunotherapeutic activity of systemically administered VSV-TAA generated T-cell responses that cleared subclinical metastatic tumors. We also showed that SABR induced weak T-cell-mediated tumor responses, which, particularly if boosted by VSV−TAA, might contribute to control of local and systemic disease. In addition, VSV−TAA therapy alone had significant effects on control of both local and metastatic tumors.

Conclusions—We have shown in the present preliminary murine study using a single tumor model that this approach represents an effective, complementary combination therapy model that addresses the need for both systemic and local control in oligometastatic melanoma.

Introduction

Oligometastasis describes a state in the spectrum of the metastatic process in which aggressive local therapy can completely eradicate the tumor burden, leading to a potential cure (1, 2). A favorable subset of patients with oligometastases that respond to aggressive local therapy with high rates of disease control has been identified (3–6), characterized by a low metastatic burden and a long initial disease-free interval or favorable microRNA expression (7). However, most patients with oligometastasis have subclinical (microscopic) widely spread metastatic disease. Further advances in the treatment of oligometastasis require either improvement in the sensitivity of imaging (to detect smaller deposits amenable to local therapy) or definitive systemic therapies to control subclinical disease.

Clinically, we have demonstrated high rates of local disease control and encouraging survival in oligometastatic melanoma (OM) with a combination of immunotherapy, chemotherapy, and ablative radiation therapy. With optimal ablative radiation therapeutic techniques, the local control rate of clinically apparent lesions can be 80% to 100% (8–9). However, most OM patients develop systemic progression and die of clinically occult widely spread metastatic disease, which cannot be detected using current imaging techniques and cannot be definitively managed with conventional chemotherapy and immunotherapy. In this respect, immune checkpoint inhibitor therapy has shown great promise in metastatic patients, although the response rate has been in the range of 15% to 35%, and complete responses have rarely been observed (10). Therefore, alternative treatment options are needed to improve control of subclinical disease to complement ablative radiation therapy in OM.

We have previously demonstrated that intravenous administration of vesicular stomatitis virus (VSV) expressing tumor-associated antigens (TAAs) leads to a systemic immune response capable of effectively clearing established tumors in mice (11–18). Tumor regression was associated with the priming of antigen-specific T-cell responses induced by the systemic administration of VSV−TAA and did not result from oncolysis by virus reaching the tumor sites (15, 18). Furthermore, recent studies have demonstrated that VSV has been safely used as a vaccine in humans (19).

Stereotactic ablative radiation therapy (SABR) is a precisely targeted, high-dose radiation modality that can lead to high rates of local control (9, 20). In addition, clinical and

preclinical data have suggested that ablative radiation therapy can also be immunostimulatory as an in situ vaccine (21–24). Moreover, low-dose total body irradiation (TBI) acts as a significant immunologic adjuvant by depleting inhibitory macrophages and regulatory T cells, facilitating intratumoral lymphocyte accumulation and stimulating the immune system with the release of gut-derived lipopolysaccharide (25–27).

In the present study, we reasoned on the basis of this previous evidence that the combination of systemic VSV-mediated antigen delivery with single-fraction, high-dose radiation therapy would be an effective treatment in the context of OM. Using a model of OM in C57BL/6 immunocompetent mice, we show that the combination of SABR and systemically administered VSV−TAA viral immunotherapy is able to treat both well-established local tumor and eradicate widespread metastases.

Methods and Materials

Cells and viruses

B16-OVA melanoma cells were derived from the B16.F1 clone transfected with pcDNA3.1OVA. B16-OVA were grown in Dulbecco's modified Eagle's medium supplemented with 10% fetal calf serum and 5 mg/mL G418 (Mediatech, Manassas, VA). All cell lines were free of *Mycoplasma* infection. VSV−OVA was generated as previously described (11).

In vivo studies

All intravenously administered cells or virus were delivered through the tail vein. To assess T-cell activation, C57BL/6 mice (Jackson Laboratory, Bar Harbor, ME), at 6 to 8 weeks of age, were injected with 5×10^5 B16-OVA cells in 100 μL of phosphate-buffered saline (PBS) subcutaneously in the hind limb. The mice were also injected (8 days after challenge) intravenously with 1×10^6 naive OT-1 T cells, which express a transgenic T-cell receptor specific for the OVA-derived SIINFEKL epitope presented by B16-OVA (28, 29).

To model local disease, 4×10^5 B16-OVA cells (100 μL of PBS) were injected into the hind limb. For oligometastatic disease, 5×10^4 cells were injected subcutaneously in the hind limb to establish local tumor. Next, to establish systemic tumors, the mice bearing subcutaneous tumors were injected intravenously with either a "low" burden (4×10^4) or a "high" burden (4×10^5) of B16-OVA cells (100 μL of PBS). For all therapy experiments, the mice were assigned randomly to the different treatment groups. For mice treated with radiation alone, a clinical linear accelerator was used to deliver SABR in a single 20-Gy fraction, at a dose rate of 600 cGy/min using 12-MeV electrons with a 1-cm bolus to the hind limb. Proper tumor localization was confirmed with megavoltage portal images before and after treatment. Electrons were chosen to facilitate improved dose distribution in the build-up region. Dose delivery was confirmed using Gafchromic EBT3 film. Alternatively, the mice were treated with VSV−OVA viral immunotherapy alone, delivered intravenously at 5×10^6 plaque-forming units (PFU)/100 μL PBS. Finally, some mice were treated with a combination of both therapies using the schedules shown in Figures 1A, 2A, and 3A. For the experiment shown in Figure 4, the mice were treated with either SABR (day 7) or

intravenous VSV−OVA (days 8 and 9), or both (with the same dose of radiation and VSV −OVA).

Total body irradiation (TBI) (2 Gy) was delivered to the midplane using a cesium irradiator. For depletion studies, anti-CD8, anti-CD4, or anti-asialo ganglio-N-tetraosylceramide (GM1) antibodies were delivered by intraperitoneal administration twice weekly, as previously described (13), beginning 1 week before treatment and continuing for the next 6 weeks. A control group for no depletion was treated with an isotype control antibody.

The subcutaneous tumors were measured 3 times weekly, and the mice were killed when the tumor had reached 1 cm in any dimension or they showed signs of distress. The presence of systemic tumor was monitored at death by conducting a complete necropsy, taking note of the presence of metastatic disease. For local therapy, 2 sequential increases in tumor size were considered disease progression. For the oligometastatic model, progression was defined as 2 sequential increases in subcutaneous tumor size or distress, with necropsy confirmation of metastases. For disease-free survival, the mice that were killed with obvious signs of VSV toxicity (hind limb paralysis or neural distress) or without necropsy-confirmed malignancy were censored from the survival analysis to differentiate between death from tumor progression and death from treatment-related toxicity. Kaplan-Meier estimates were used for the overall survival and disease-free survival estimates.

In vitro splenic T-cell reactivation and enzyme-linked immunosorbent assay

The spleen and lymph node cells were prepared as previously described (14–18) after harvesting at death from mice in the therapy experiments (Figs. 1–3) or 15 days after tumor challenge (Fig. 4). Next, 1×10^6 cells were stimulated with peptide OVA (SIINFEKL) or mouse glycoprotein 100 (gp100) (EGSRNQDWL) for 48 hours, and the cell-free supernatants were tested by enzyme-linked immunosorbent assay for interferon-γ (BD Biosciences, San Jose, CA).

Flow cytometry

The tumors and spleens were prepared for flow cytometry as previously described (14–18). Intracellularly stained cells were first stimulated using SIINFEKL peptide for 4 hours in the presence of Golgi Plug before being extracellularly stained. The cells were then fixed and permeabilized for intracellular staining using the Cytofix/Cytoperm Kit (BD Biosciences). Primary anti-CD8b and anti-interferon-γ antibodies were obtained from eBioscience (San Diego, CA). The samples were analyzed using FlowJo software (FlowJo, Ashland, OR).

Statistical analysis

Data were analyzed using the appropriate statistical tests: the Mann-Whitney *U* test or unpaired *t* tests for quantitative enzyme-linked immunosorbent assay and FACS analysis, respectively, and log-rank tests for the survival analysis. All statistical analyses were conducted using GraphPad Prism software (GraphPad Software, La Jolla, CA). Statistical significance was determined at $P \leq .05$ and corrected for multiple comparisons using Bonferroni's correction.

Results

Viral immunotherapy with ablative radiation therapy maximizes local control

We tested the efficacy of SABR, intravenous VSV−OVA, SABR and intravenous VSV−OVA together, and TBI against locally established tumor (Fig. 1A). We used a single suboptimal dose of 20 Gy to uncover any synergy between radiation therapy and viral immunotherapy. All mice treated with SABR developed moist desquamation within the irradiated field uniformly 3 weeks after treatment, with subsequent significant tissue fibrosis in the subsequent months. Either treatment alone generated statistically significant improvements in the median time to tumor progression compared with no treatment, which was our control group in this experiment. Systemic VSV−OVA immunotherapy targeting the OVA TAA was at least as effective at local tumor control as was SABR (Fig. 1B). The combination of SABR with VSV−OVA viral immunotherapy was significantly more efficacious than either monotherapy (median time to tumor progression with VSV+SABR 59 days compared with 31 days with VSV alone [$P = .04$] and 22 days with SABR alone [$P = .0005$]). The combination of SABR with viral immunotherapy consistently generated a trend of improved overall survival compared with either alone ($P = .01$ compared with SABR alone), although this did not reach significance when accounting for multiple comparisons (Fig. 1C). The addition of TBI to SABR+VSV−TAA did not add further therapeutic gain to either the growth delay of the tumors (Fig. 1B) or survival (Fig. 1C). Thus, both high-dose local radiation therapy and systemic VSV−TAA controlled local tumor growth, and combining them improved treatment efficacy.

Viral immunotherapy and ablative radiation therapy leads to long-term cure of OM

The mice were challenged with either a “low” or a “high” burden of oligometastatic disease by subcutaneous and intravenous injection of tumor cells. In the “low” OM burden model (Fig. 2A), all treatments were significantly more effective than no treatment at controlling tumor and prolonging survival ($P<.008$; Fig. 2B,C). Although VSV+SABR significantly improved overall survival compared with SABR alone ($P<.0001$), no improvement was seen compared with VSV alone (Fig. 2D). Because of the lack of efficacy with the addition of TBI (Fig. 1B,C), TBI was not tested in this experiment. Mice treated with SABR alone were killed because of widespread metastases in one half of the treatment group. This was in contrast to the lack of any systemic disease noted in any treatment group that received VSV (Fig. 2E).

The depletion of natural killer NK and CD4+ cells in mice treated with VSV−OVA+SABR emerged as the most important for the control of local and metastatic disease. Although no CD4+-depleted mice had evidence of metastasis at death, 1 of 10 PBS treated and 6 of 7 mice depleted of NK cells had metastatic disease noted at necropsy. All mice treated with isotype control antibodies demonstrated long-term survival (>85 days), with only 1 mouse needing to be killed because of metastatic disease (Fig. 2F).

Similarly, with the “high” disease burden (Fig. 3A), VSV+SABR treatment improved local tumor control (Fig. 3B), and the combination of VSV−OVA with SABR significantly increased the actuarial disease-free survival rate to 67% after >4 months compared with 13%

with VSV−OVA and 0% with SABR alone (Fig. 3C; disease recurrence or death with any tumor present at necropsy). Furthermore, the combination therapy significantly improved overall survival compared with SABR alone ($P = .03$) but not compared with VSV alone (Fig. 3D). However, this comparison was no longer statistically significant when accounting for multiple comparisons. At 130 days, the median time to progression had not been reached after SABR+VSV−OVA. This was in contrast to 42 days for SABR alone ($P = .0008$). Superior disease-free survival compared with overall survival resulted from censoring the deaths of mice with no evidence of malignancy at necropsy. This metric accounts for deaths that resulted from disease progression rather than from treatment toxicity. Furthermore, the increased SABR-related toxicity in the combination-treated mice can be explained by the rapid death of the solely SABR-treated mice, which were killed before radiation toxicity might have developed.

In both models of oligometastatic disease, all mice receiving single modality VSV−OVA progressed first with growth of the local tumor, in contrast to progression with disseminated tumor. SABR (alone or in any combination) was highly effective at controlling local tumor such that most mice receiving single-modality SABR were killed because of progression of systemic disease before local recurrence had developed. On necropsy, the mice displayed evidence of widespread metastases, thereby validating our model of oligometastatic disease (Figs. 2E, 3E). Just as in the case with only local subcutaneous disease (Fig. 1), adding TBI to combination VSV+SABR therapy resulted in no improvement in treatment outcomes (data not shown).

High-dose radiation therapy and viral therapy activates naive T cells

Based on our previous success with using adoptive cell therapy to treat tumors and, in particular, being able to monitor the immune response to the OVA tumor antigen (13, 28), we transferred OT-1 CD8+ cells into B16-challenged mice in combination with SABR. Subcutaneous tumors were infiltrated with a significantly higher percentage of CD8+ T cells after treatment with intravenous VSV−OVA or VSV−OVA+SABR compared with the untreated mice (Fig. 4A). A higher percentage of T cells were activated after any treatment with VSV−OVA compared with no treatment or SABR alone (Fig. 4B,C). Significantly fewer tumor-infiltrating T cells were activated after treatment with SABR+VSV−OVA than in VSV−OVA treated mice (Fig. 4C), possibly because high-dose intra-tumoral radiation attenuated the function of any endogenously activated, tumor-infiltrating immune cells directly. In addition, based on our findings that B16 tumors secrete significant amounts of transforming growth factor-β and other immunosuppressive cytokines on cell killing (Kottke and Vile, unpublished data), we hypothesized that the local factors released as a result of high-dose radiation-induced cell death might also inhibit OT-I T-cell trafficking when the cells were adoptively transferred 1 day after radiation. Consistent with this, a higher percentage of splenic CD8+ T cells (outside the radiation field) were activated in the mice treated with SABR+VSV−OVA, although the difference was not statistically significant ($P = .07$ compared with VSV alone; Fig. 4D). Surprisingly, CD8+ T cells did not infiltrate tumors to any greater extent in SABR-treated mice compared with the control-treated mice (Fig. 4A) (22). In addition, SABR did not activate these CD8+ cells more than did control treatment in either tumor or spleen (Fig. 4C,D), suggesting that CD8+ cells are not the

primary driver of the antitumor immune response observed in mice treated with both SABR and VSV−OVA.

Combination viral immunotherapy induces epitope spreading

As previously observed (11), VSV−OVA primed strong T-cell responses against the virally encoded OVA TAA when administered with or without SABR (Fig. 5A). SABR primed anti-OVA T-cell responses at very low levels compared with VSV−OVA ($P = .007$), but these were greater than those in the controls (no anti-OVA responses; Fig. 5A), suggesting that SABR has small, but definite, immunotherapeutic benefits in releasing TAA for T-cell presentation and activation.

Significantly, VSV−OVA primed T-cell responses against a truly endogenous, self-TAA, gp100 (30), expressed by B16-OVA melanomas, in most mice ($P = .01$ compared with control; Fig. 5B). Similar anti-gp100 T-cell responses were also generated in some mice treated with SABR and VSV−OVA. Also, SABR alone generated weaker, but detectable, anti-gp100 responses (Fig. 5B). Thus, SBRT CD8+ T-cell activation plays a role in the improved immunologic control of OM but represents only 1 factor in a complex multifactorial process that remains to be elucidated.

Discussion

Our current experiments arose from 2 observations. The first was that systemic VSV expressing TAA generated T-cell responses that could clear established tumors (11, 12, 14–18). The second key observation was that single-fraction ablative radiation therapy is very effective at controlling local disease (3–6). Therefore, we reasoned that the combination of these 2 strategies would be effective in the context of oligometastatic disease and hypothesized that SABR and VSV viral immunotherapy would synergize to control all aspects of OM. We also hypothesized that VSV−TAA-mediated priming of anti-tumor T-cell responses would help the local effects of SABR to clear residual, radiation-resistant tumor. Moreover, we sought to test the hypothesis that SABR might itself provide an immunogenic form of tumor cell death that would prime anti-tumor T-cell responses against both residual local and metastatic tumor (21, 23, 24, 31).

We have shown that local SABR combined with systemic viral immunotherapy cured (long-term survival with local tumor eradicated) more than 80% of mice with oligometastatic disease when treatment was administered with a low initial tumor burden (Fig. 2). Both VSV−TAA and SABR had significant efficacy against local, established subcutaneous tumor (Fig. 1). When treated with SABR alone, the oligometastatic disease of mice was largely controlled at the local site but with necropsy-confirmed disseminated metastatic disease. In contrast, mice harboring oligometastatic disease treated only with VSV−TAA developed rapid progression at the local tumor site (Figs. 2 and 3). These data are consistent with a model in which SABR effectively controls the local tumor, and systemic VSV−TAA primes T-cell responses to control metastatic disease. Furthermore, the data from our depletion study suggested that CD4 and NK cells exert an immunologic effect on tumor that warrants additional investigation about their precise role (Fig. 2).

In early experiments, antitumor therapy was sometimes associated with high levels of viral toxicity, principally hind limb paralysis and/or neural distress. However, with refinement of our experimental techniques (ie viral purification), this was reduced to <10% of mice experiencing VSV-related toxicity. Future experiments will address this issue with the use of more heavily attenuated strains of VSV in which additional safety genes (eg interferon-β) or mutations are expressed (32, 33). Furthermore, simple interventions such as antipyretics, antiemetics, and sophisticated radiation therapeutic techniques available to human trials might largely eliminate other toxicities.

Consistent with our previous studies (11), VSV−OVA primed a substantial tumor-infiltrating CD8+ T-cell response (Fig. 4). Systemic virus significantly enhanced the levels of activated tumor-infiltrating T cells compared with controls, confirming the immunotherapeutic effects of this treatment. The addition of SABR to VSV−OVA somewhat reduced the activity of the infiltrating CD8+ T cells but showed a trend toward amplification of their systemic activity, consistent with the local cytotoxic effects of high-dose radiation on tumor-infiltrating cells (Fig. 4C). VSV-encoding OVA was significantly more effective at priming naive CD8+ T cells in vivo than was tumor-derived OVA released from SABR-mediated tumor killing (Fig. 4). After correcting for multiple comparisons, only the addition of VSV therapy to radiation therapy resulted in statistically significant improvements in CD8+ cell priming.

This was also true in our OM model, in which VSVOVA was significantly more effective at priming endogenous T-cell responses against OVA than was SABR (Fig. 5). In addition, the antitumor effects of systemic viral immunotherapy led to priming of T-cell responses against the endogenous melanoma-associated TAA gp100 (30) (Fig. 5). Presumably, this epitope spreading (34) was mediated by in vivo killing of tumor cells by the anti-OVA T-cell responses primed by VSV−OVA, which then allowed immunogenic release of the endogenous TAA for additional T-cell priming. Our immune depletion studies demonstrated significant contributions of CD8+, CD4+, and NK cells to the efficacy of the combination therapy (Fig. 2F). These data help to explain the finding of no significant difference in the anti-OVA, or gp100, CD8+ T-cell responses generated by VSV+SABR compared with VSV alone (Figs. 4 and 5), showing that the synergistic effects of the combination therapy worked through multicomponent immunologic mechanisms in vivo.

Although priming of anti-TAA T-cell responses was consistently greater with VSV−OVA than with SABR, we observed a trend toward the priming of T-cell responses against both foreign OVA and the self-TAA gp100 by SABR alone, supporting a possible role for radiation in causing immunogenic tumor cell death (22) (Fig. 5). However, the combination of SABR and VSV−TAA therapy did not add significant levels of additional T-cell priming, suggesting that VSV−TAA might be the dominant immunologic priming component of this therapy. This raises the possibility that 1 aspect of the excellent overall therapy for OM results from an immunotherapeutic prime or boost effect. In this scenario, SABR primes low-level T-cell responses against a variety of TAAs (Fig. 5). Next, VSV−TAA subsequently boosts that T-cell response against a variety of TAAs expressed in local and metastatic disease through epitope spreading. In the present study, we have demonstrated a small role of CD8+ T cells in the survival benefit of VSV+SABR combination treatment and a larger role for CD4 and NK cells. These data suggest that additional improvements will be possible

through the combination of VSV−TAA+SABR with additional treatment, such as immune checkpoint inhibitors (35, 36). In the present experiments, we used the B16-OVA/VSV −OVA tumor model, because it allowed us to closely monitor the immunologic sequelae of SABR and VSV−TAA therapies, both separately and together. In the treatment of patient tumors, immune reactivity against multiple weak TAAs will be required to ensure effective tumor control and prevent tumor escape. Therefore, experiments are underway using VSV-cDNA libraries expressing a wide variety of TAAs, such as we have previously described (14, 15), combined with SBRT to address this specific issue.

Conclusions

We have shown that a combination of highly targeted single-fraction radiation therapy can be combined with systemic viral immunotherapy to treat OM. This approach represents an effective, complementary combination therapy model that is readily translatable to the clinic and that can be further combined with additional immune modulator therapies.

Acknowledgments

We thank Toni Higgins for expert secretarial assistance. This work was funded by The Richard M. Schulze Family Foundation, the Mayo Foundation, Cancer Research UK, the National Institutes of Health (Grants R01CA107082, R01CA130878, R01CA132734, and R01CA175386-01A1), the European Research Council, the University of Leeds, the University of Minnesota/Mayo Foundation Partnership (MNP#14.14), and a grant from Terry and Judith Paul. K.J.H. received support from the ICR/RM NIHR Biomedical Research Centre.

References

1. Hellman S, Weichselbaum RR. Oligometastases. J Clin Oncol. 1995; 13:8–10. [PubMed: 7799047]
2. Niibe Y, Chang JY. Novel insights of oligometastases and oligorecurrence and review of the literature. Pulm Med. 2012; 2012:261096. [PubMed: 22966429]
3. Patchell RA, Tibbs PA, Walsh JW, et al. A randomized trial of surgery in the treatment of single metastases to the brain. N Engl J Med. 1990; 322:494–500. [PubMed: 2405271]
4. Andrews DW, Scott CB, Sperduto PW, et al. Whole brain radiation therapy with or without stereotactic radiosurgery boost for patients with one to three brain metastases: Phase III results of the RTOG 9508 randomised trial. Lancet. 2004; 363:1665–1672. [PubMed: 15158627]
5. Johnson PW, Sydes MR, Hancock BW, et al. Consolidation radiotherapy in patients with advanced Hodgkin's lymphoma: Survival data from the UKLG LY09 randomized controlled trial (ISRCTN97144519). J Clin Oncol. 2010; 28:3352–3359. [PubMed: 20498402]
6. Wolden SL, Chen L, Kelly KM, et al. Long-term results of CCG 5942: A randomized comparison of chemotherapy with and without radiotherapy for children with Hodgkin's lymphoma–A report from the Children's Oncology Group. J Clin Oncol. 2012; 30:3174–3180. [PubMed: 22649136]
7. Lussier YA, Xing HR, Salama JK, et al. MicroRNA expression characterizes oligometastasis(es). PLoS One. 2011; 6:e28650. [PubMed: 22174856]
8. Greco C, Zelefsky MJ, Lovelock M, et al. Predictors of local control after single-dose stereotactic image-guided intensity-modulated radiotherapy for extracranial metastases. Int J Radiat Oncol Biol Phys. 2011; 79:1151–1157. [PubMed: 20510537]
9. Stinauer MA, Kavanagh BD, Schefter TE, et al. Stereotactic body radiation therapy for melanoma and renal cell carcinoma: Impact of single fraction equivalent dose on local control. Radiat Oncol. 2011; 6:34. [PubMed: 21477295]
10. Ott PA, Hodi FS, Robert C. CTLA-4 and PD-1/PD-L1 blockade: New immunotherapeutic modalities with durable clinical benefit in melanoma patients. Clin Cancer Res. 2013; 19:5300–5309. [PubMed: 24089443]

11. Diaz RM, Galivo F, Kottke T, et al. Oncolytic immunovirotherapy for melanoma using vesicular stomatitis virus. Cancer Res. 2007; 67:2840–2848. [PubMed: 17363607]
12. Wongthida P, Diaz RM, Pulido C, et al. Activating systemic T-cell immunity against self tumor antigens to support oncolytic virotherapy with vesicular stomatitis virus. Hum Gene Ther. 2011; 22:1343–1353. [PubMed: 21366404]
13. Rommelfanger DM, Wongthida P, Diaz RM, et al. Systemic combination virotherapy for melanoma with tumor antigen-expressing vesicular stomatitis virus and adoptive T-cell transfer. Cancer Res. 2012; 72:4753–4764. [PubMed: 22836753]
14. Kottke T, Errington F, Pulido J, et al. Broad antigenic coverage induced by viral cDNA library-based vaccination cures established tumors. Nat Med. 2011; 2011:854–859. [PubMed: 21685898]
15. Pulido J, Kottke T, Thompson J, et al. Using virally expressed melanoma cDNA libraries to identify tumor-associated antigens that cure melanoma. Nat Biotechnol. 2012; 30:337–343. [PubMed: 22426030]
16. Boisgerault N, Kottke T, Pulido J, et al. Functional cloning of recurrence-specific antigens identifies molecular targets to treat tumor relapse. Mol Ther. 2013; 21:1507–1516. [PubMed: 23752316]
17. Zaidi S, Blanchard M, Shim K, et al. Mutated BRAF emerges as a major effector of recurrence in a murine melanoma model after treatment with immunomodulatory agents. Mol Ther. 2014; 23:845–856. [PubMed: 25544599]
18. Alonso-Camino V, Rajani K, Kottke T, et al. The profile of tumor antigens which can be targeted by immunotherapy depends upon the tumor's anatomical site. Mol Ther. 2014; 22:1936–1948. [PubMed: 25059678]
19. Lai L, Davey R, Beck A, et al. Emergency postexposure vaccination with vesicular stomatitis virus-vectored *Ebola* vaccine after needle-stick. JAMA. 2015; 313:1249–1255. [PubMed: 25742465]
20. Tree AC, Khoo VS, Eeles RA, et al. Stereotactic body radiotherapy for oligometastases. Lancet Oncol. 2013; 14:e28–e37. [PubMed: 23276369]
21. Levy A, Chargari C, Cheminant M, et al. Radiation therapy and immunotherapy: Implications for a combined cancer treatment. Crit Rev Oncol Hematol. 2013; 85:278–287. [PubMed: 23036459]
22. Lee Y, Auh SL, Wang Y, et al. Therapeutic effects of ablative radiation on local tumor require CD8+ T cells: Changing strategies for cancer treatment. Blood. 2009; 114:589–595. [PubMed: 19349616]
23. Apetoh L, Ghiringhelli F, Tesniere A, et al. Toll-like receptor 4-dependent contribution of the immune system to anticancer chemotherapy and radiotherapy. Nat Med. 2007; 13:1050–1059. [PubMed: 17704786]
24. Golden EB, Frances D, Pellicciotta I, et al. Radiation fosters dose-dependent and chemotherapy-induced immunogenic cell death. Oncoimmunology. 2014; 3:e28518. [PubMed: 25071979]
25. Paulos CM, Wrzesinski C, Kaiser A, et al. Microbial translocation augments the function of adoptively transferred self/tumor-specific CD8+ T cells via TLR4 signaling. J Clin Invest. 2007; 117:2197–2204. [PubMed: 17657310]
26. Restifo NP, Dudley ME, Rosenberg SA. Adoptive immunotherapy for cancer: Harnessing the T cell response. Nat Rev Immunol. 2012; 12:269–281. [PubMed: 22437939]
27. Rosenberg SA. Cell transfer immunotherapy for metastatic solid cancer—What clinicians need to know. Nat Rev Clin Oncol. 2011; 8:577–585. [PubMed: 21808266]
28. Kaluza KM, Thompson J, Kottke T, et al. Adoptive T cell therapy promotes the emergence of genomically altered tumor escape variants. Int J Cancer. 2012; 131:844–854. [PubMed: 21935923]
29. Hogquist KA, Jameson SC, Health WR, et al. T cell receptor antagonistic peptides induce positive selection. Cell. 1994; 76:17–27. [PubMed: 8287475]
30. Overwijk WW, Theoret MR, Finkelstein SE, et al. Tumor regression and autoimmunity after reversal of a functionally tolerant state of self-reactive CD8+ T cells. J Exp Med. 2003; 198:569–580. [PubMed: 12925674]
31. Lugade AA, Moran JP, Gerber SA, et al. Local radiation therapy of B16 melanoma tumors increases the egneration of tumor antigen specific effector cells that traffic to the tumor. J Immunol. 2005; 174:7516–7523. [PubMed: 15944250]

32. Stojdl DF, Lichty BD, ten Oever BR, et al. VSV strains with defects in their ability to shutdown innate immunity are potent systemic anticancer agents. Cancer Cell. 2003; 4:263–275. [PubMed: 14585354]

33. Willmon CL, Saloura V, Fridlender ZG, et al. Expression of IFN-beta enhances both efficacy and safety of oncolytic vesicular stomatitis virus for therapy of mesothelioma. Cancer Res. 2009; 69:7713–7720. [PubMed: 19773437]

34. Disis ML. Immunologic biomarkers as correlates of clinical response to cancer immunotherapy. Cancer Immunol Immunother. 2011; 60:433–442. [PubMed: 21221967]

35. Dovedi SJ, Adlard AL, Lipowska-Bhalla G, et al. Acquired resistance to fractionated radiotherapy can be overcome by concurrent PD-L1 blockade. Cancer Res. 2014; 74:5458–5468. [PubMed: 25274032]

36. Zeng J, See AP, Phallen J, et al. Anti-PD-1 blockade and stereotactic radiation produce long-term survival in mice with intracranial gliomas. Int J Radiat Oncol Biol Phys. 2013; 86:343–349. [PubMed: 23462419]

Summary

We have shown that stereotactic ablative radiation therapy (SABR) can be combined with systemically administered vesicular stomatitis virus expressing a tumor-associated antigen to enhance survival in a model of oligometastatic melanoma. SABR controlled the local tumor through direct cell ablation, and systemic vesicular stomatitis virus-tumor-associated antigen generated T-cell responses that cleared the metastatic tumors. This preclinical approach represents an effective, complementary combination therapy model that can be further combined with additional immune modulator therapies.

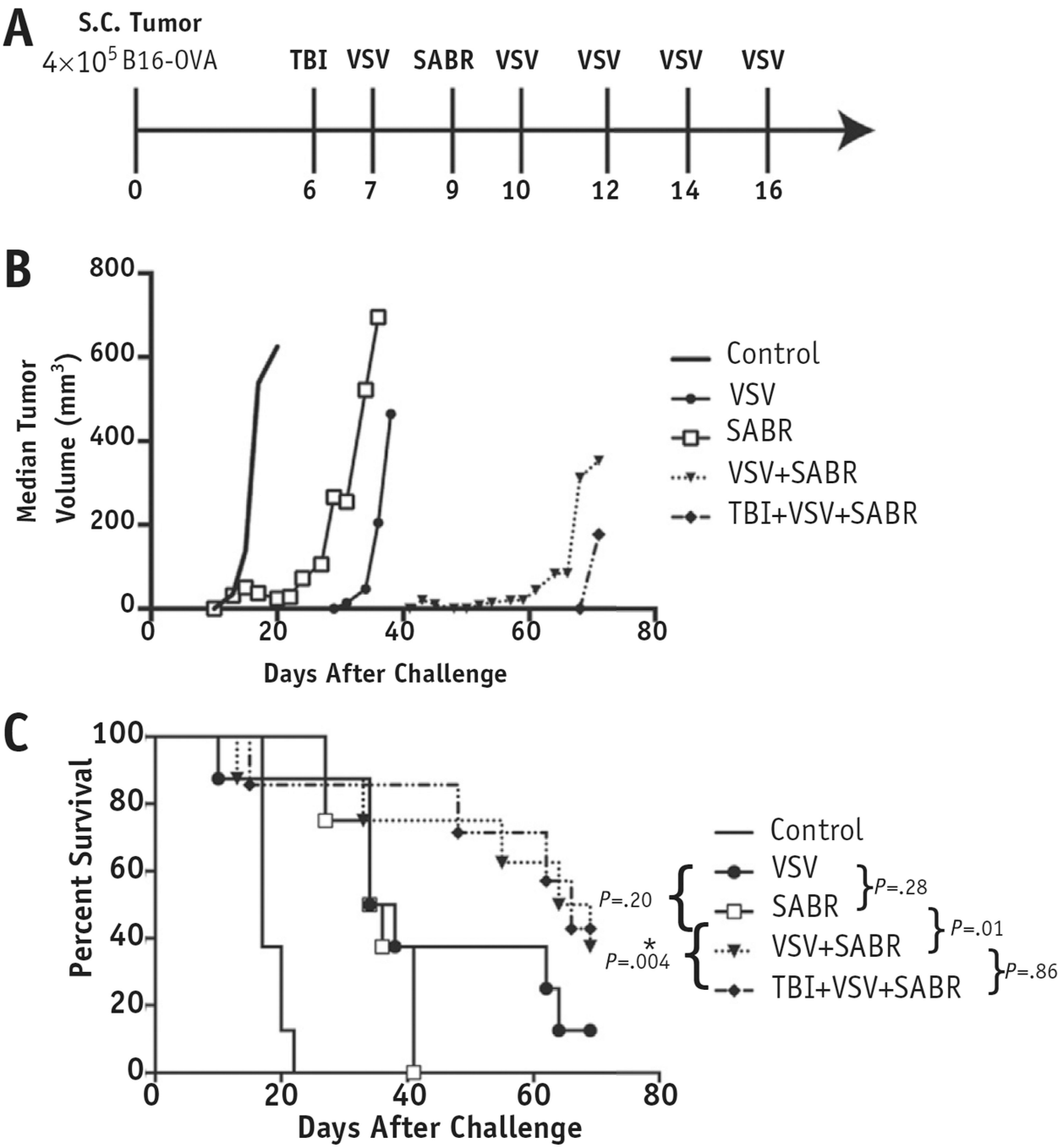

Fig. 1.

Combination viral immunotherapy and stereotactic ablative radiation therapy (SABR) delayed progression of local tumor and improved survival trends. (A) C57BL/6 mice (n = 8) injected subcutaneously in the lower limb with 4×10^5 B16-OVA cells received either 2 Gy total body irradiation (TBI) or 20 Gy radiation therapy, or both, at the times indicated. Treatment with intravenous vesicular stomatitis virus (VSV)-OVA (5×10^6 plaque-forming units) began on day 7 after tumor challenge and was continued 3 times weekly for ≤5 doses. (B) Median tumor volumes for each treatment group. (C) Kaplan-Meier survival curve

comparing overall survival among the treatment groups. Median time to tumor progression with VSV+SABR was 59 days compared with 31 days with VSV alone ($P = .04$) and 22 days with SABR alone [$P = .0005$]). P values shown are for individual comparisons among groups. The threshold for significance when accounting for multiple comparisons was $P < .005$ ($^{*}P < .005$). *Abbreviation:* S.C. = subcutaneous.

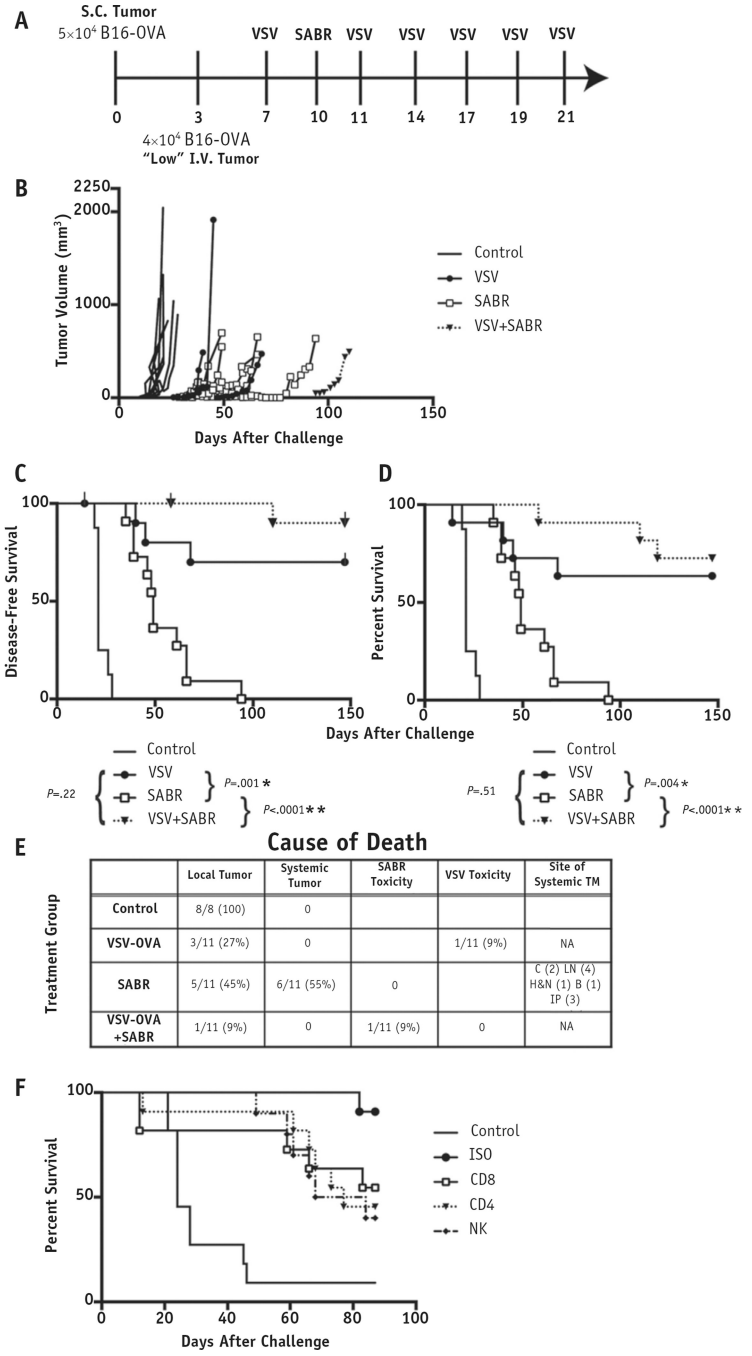

	Local Tumor	Systemic Tumor	SABR Toxicity	VSV Toxicity	Site of Systemic TM
Control	8/8 (100)	0			
VSV-OVA	3/11 (27%)	0		1/11 (9%)	NA
SABR	5/11 (45%)	6/11 (55%)	0		C (2) LN (4) H&N (1) B (1) IP (3)
VSV-OVA +SABR	1/11 (9%)	0	1/11 (9%)	0	NA

Fig. 2.

Combination systemic viral immunotherapy and radiation therapy controlled oligometastatic disease. (A) Mice (n = 8 control; n = 11 treatment) were challenged with "low"-burden oligometastatic B16-OVA. Treatment was delivered at the times shown. (B) Individual tumor growth curves for mice harboring oligometastatic disease receiving the treatments shown. Kaplan-Meier curves for (C) disease-free survival and (D) overall survival. Tick marks indicate mice censored for treatment toxicity. (E) Cause of death for each mouse, including the anatomic site of metastatic disease. (F) Kaplan-Meier survival curve for mice (n = 11)

treated with vesicular stomatitis virus (VSV)+stereotactic ablative radiation therapy (SABR) and depleted the immune cell subsets shown. *P* values shown are for individual comparisons among groups. The threshold for significance accounting for multiple comparisons was $P < .008$ (*$P < .008$, **$P < .001$). *Abbreviations:* B = bone; C = chest; Control = mice with no treatment; H&N = head and neck; IP = intraperitoneal; ISO = mice treated with an isotype control antibody as a control for no depletion; LV = low volume; NA = not applicable; S.C. = subcutaneous; TM = tumor metastases.

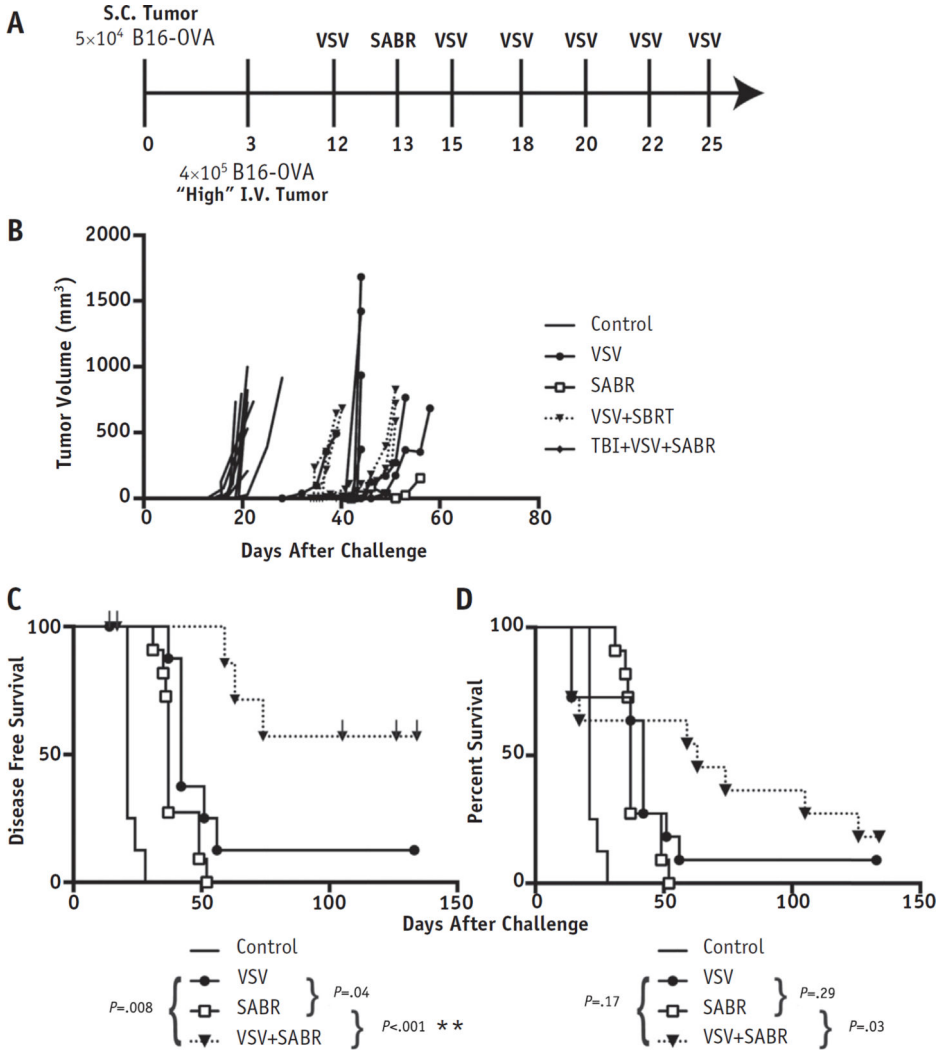

E

Cause of Death

Treatment Group	Local Tumor	Systemic Tumor	SABR Toxicity	VSV Toxicity	Site of Systemic TM
Control	8/8 (100)	0			NA
VSV-OVA	7/11 (63%)	0		3/11 (27%)	NA
SABR	0	11/11 (100%)	0		C (7) S.C (2) H&N (2) B (2) IP (2)
VSV-OVA +SABR	0	2/11 (18%)	3/11 (27%)	4/11 (36%)	C (2)

Fig. 3.

Combination systemic viral immunotherapy and radiation therapy improved outcomes in oligometastatic disease. (A) Mice (n = 8 control; n=11 treatment) were challenged with intravenous (I.V.) "high"-burden oligometastatic B16-OVA. (B) Individual tumor growth curves for mice harboring oligometastatic disease receiving the treatments shown. Kaplan-Meier curves for (C) disease-free survival and (D) overall survival. Tick marks indicate mice censored for treatment toxicity. (E) Cause of death of each mouse, including the anatomic site of metastatic disease. *P* values shown are for individual comparisons among groups. The

threshold for significance accounting for multiple comparisons was $P < .008$ (*$P < .008$, **$P < .001$). *Abbreviations:* C = chest; Control = mice with no treatment; H&N = head and neck; IP = intraperitoneal; NA = not applicable; S.C. = subcutaneous; TM = tumor metastases.

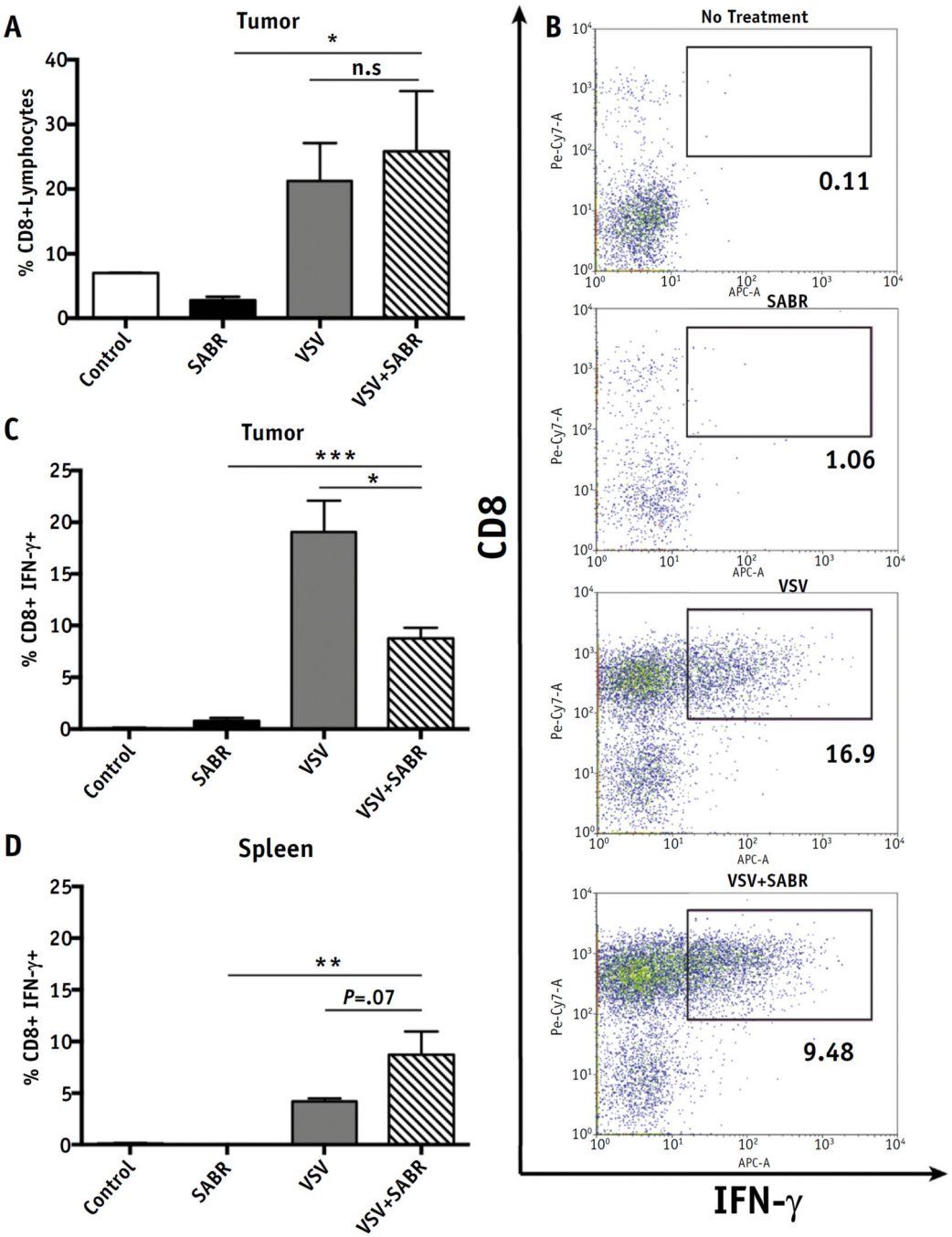

Fig. 4.

Effect of therapy on activation of naive T cells. Mice were administered naive OT-1 T cells (1×10^6 cells) on day 8 after tumor challenge (n = 3). Flow cytometry was performed 15 days after tumor challenge on explanted tumors and spleens of mice harboring local disease treated with either 20 Gy of stereotactic ablative radiation therapy (SABR) or 2 doses of vesicular stomatitis virus (VSV)-OVA (5×10^6 plaque-forming units), or both. (A) Number of CD8+ T cells as a percentage of tumor-infiltrating lymphocytes from similarly sized tumors (~0.2 cm in diameter). (B) Dot plots of representative tumors from each group

displaying percentage of CD8+ interferon (IFN)-γ+ lymphocytes. Intracellular flow cytometry results displaying percentage of CD8+ tumor-infiltrating lymphocytes producing IFN-γ (C) and splenocytes (D). Mean percentage plotted with standard deviation (*$P < .05$, **$P < .01$, ***$P < .001$).

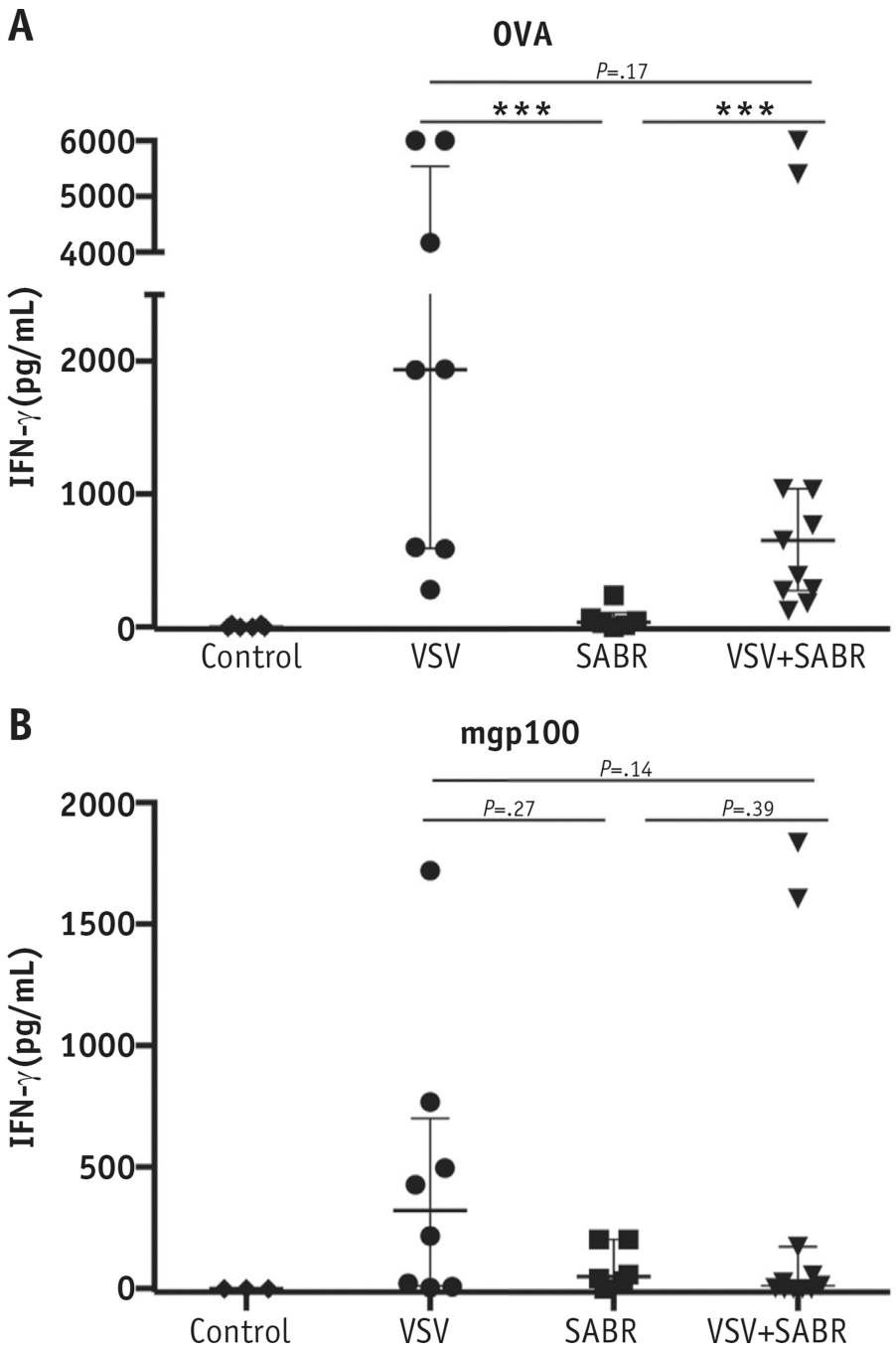

Fig. 5.

Combination vesicular stomatitis virus (VSV) and stereotactic ablative radiation therapy (SABR) results in interferon (IFN)-γ splenocyte responses to tumor-associated antigens. Splenocyte antigen recall response from mice of each treatment group (n = 6–11 per group) was evaluated using IFN-γ enzyme-linked immunosorbent assay. Freshly explanted splenocytes were stimulated with (A) SIINFEKL peptide or (B) mouse glycoprotein (mgp)

100 peptide for 48 hours. Median and interquartile range shown. Each point represents 1 mouse (*$P < .05$, **$P < .01$, ***$P < .001$).